Journal of Histochemistry & Cytochemistry 2015, Vol. 63(6) 427–437

DOI: 10.1369/0022155415580396
jhc.sagepub.com
SAGE

Structural Analysis of Alterations in Zebrafish Muscle Differentiation Induced by Simvastatin and Their Recovery with Cholesterol

Laise M. Campos, Eduardo A. Rios, Victor Midlej, Georgia C. Atella, Suzana Herculano-Houzel, Marlene Benchimol, Claudia Mermelstein, and Manoel Luís Costa

Instituto de Ciências Biomédicas, Universidade Federal do Rio de Janeiro, RJ, Brazil (LMC,EAR,SHH,CM,MLC); Laboratório de Ultraestrutura Celular, Universidade Santa Úrsula, RJ, Brazil (VM,MB); and Instituto de Bioquímica Médica, Universidade Federal do Rio de Janeiro, RJ, Brazil (GCA)

Summary

In vitro studies show that cholesterol is essential to myogenesis. We have been using zebrafish to overcome the limitations of the in vitro approach and to study the sub-cellular structures and processes involved during myogenesis. We use simvastatin—a drug widely used to prevent high levels of cholesterol and cardiovascular disease—during zebrafish skeletal muscle formation. Simvastatin is an efficient inhibitor of cholesterol synthesis that has various myotoxic consequences. Here, we employed simvastatin concentrations that cause either mild or severe morphological disturbances to observe changes in the cytoskeleton (intermediate filaments and microfilaments), extracellular matrix and adhesion markers by confocal microscopy. With low-dose simvastatin treatment, laminin was almost normal, and alpha-actinin was reduced in the myofibrils. With high simvastatin doses, laminin and vinculin were reduced and appeared discontinuous along the septa, with almost no myofibrils, and small amounts of desmin accumulating close to the septa. We also analyzed sub-cellular alterations in the embryos by electron microscopy, and demonstrate changes in embryo and somite size, septa shape, and in myofibril structure. These effects could be reversed by the addition of exogenous cholesterol. These results contribute to the understanding of the mechanisms of action of simvastatin in muscle cells in particular, and in the study of myogenesis in general. (J Histochem Cytochem 63:427–437, 2015)

Keywords

cell adhesion, desmin, myofibrils, myogenesis, simvastatin, zebrafish embryos

Introduction

The study of myogenesis is necessary to comprehend the basic biological mechanisms of muscle diseases and for the development of potential treatment strategies. In vitro studies have shown in detail the cellular structures involved in myogenesis and that cholesterol has structural and signaling effects in myogenesis; but these tests were performed using muscle cultures. The interpretation of these studies and their extrapolation for human systems are thus restricted, because cell cultures are two-dimensional simplifications that can be quite different from the actual muscle formation in the embryo. We have been using zebrafish to overcome these limitations and to study the sub-cellular structures and processes during myogenesis. We decided to study the

Received for publication October 27, 2014; accepted March 11, 2015.

Supplementary material for this article is available on the *Journal of Histochemistry & Cytochemistry* Web site at http://jhc.sagepub.com/supplemental.

Corresponding Author:
Manoel Luís Costa, Laboratorio de Diferenciação Muscular e Citoesqueleto, Instituto de Ciências Biomédicas, Universidade Federal do Rio de Janeiro, Centro de Ciências da Saúde, Av. Carlos Chagas s/n, RJ 21949-590, Brazil.
E-mail: manoelluiscosta@ufrj.br

effects of simvastatin in zebrafish skeletal muscle formation. Simvastatin is an efficient inhibitor of cholesterol synthesis, used to prevent high levels of cholesterol and cardiovascular disease, which causes various myotoxic consequences. Our previous results have shown that high levels of simvastatin induce structural damage whereas low doses induce minor structural changes, impaired movement and reduced heart beating (unpublished observations). Since the muscle mechanical function is based on its structure, we decided to study in detail the distribution of the cellular components involved in myogenesis.

Myogenesis begins with the commitment of precursor cells to myoblasts, a process mediated by morphogens that induce the expression of muscle master switch genes to regulate the expression of muscle-specific proteins. These myoblasts elongate and fuse to form multi-nucleated and striated myotubes, which are filled with contractile protein systems. These myofibrils are composed of interdigitating actin microfilaments and myosin II filaments, distributed periodically in sarcomeres, with associated regulating proteins (Clark et al. 2002). The assembly of myofibrils involves the attachment of precursor structures to the membrane in regions with integral membrane proteins, such as integrins and dystroglycans, which will link the cytoskeleton to the extracellular matrix. It was previously shown in vitro that the assembly of myofibrils depends on their ability to develop tension (Engler et al. 2004). Cell-cell adhesion is also important in myogenesis, particularly for muscle cell fusion, where cells have to come in close contact. The role of membrane proteins can be demonstrated by the progressive change in integrin and cadherin isoforms during myogenesis (Kaufmann et al. 1999). It is reasonable to say that muscle differentiation is based on cytoskeleton and adhesion adaptations, which can be studied as changes in the distribution of key molecules during myogenesis (Costa 2014).

The adhesion sites are part of the specialized areas of the membrane called membrane microdomains. The knockdown of muscle-specific caveolin causes the disorganization of membrane microdomains and muscle dystrophy (Galbiati et al. 2001). We have previously demonstrated that disorganization of lipid rafts by treatment with the cholesterol-sequestering drug methyl-beta-cyclodextrin leads to alterations in the structural and signaling aspects of myogenesis (Mermelstein et al. 2005; Mermelstein et al. 2007; Portilho et al. 2012).

We chose to study the role of cholesterol and microdomains in the zebrafish embryo, an integrated model of myogenesis, which allowed us to study muscle development in three dimensions. Zebrafish embryos are transparent, and we and others have previously characterized several aspects of its myogenesis, particularly with respect to cytoskeletal and adhesion structures (Costa et al. 2002; Costa et al. 2008; Henry et al. 2005). We chose to use simvastatin because it is widely used in the clinical treatment of high cholesterol and therefore the results of this research will be more useful to the study of diseases. Simvastatin blocks cholesterol synthesis by inhibiting HMG-CoA reductase (Tobert 2003).

Other studies have shown structural effects of simvastatin in zebrafish but they did not study the affected structures in detail. The works of Hanai et al. (2007) and Cao et al. (2009) studied statin-induced muscle toxicity in zebrafish embryos. Using low magnification imaging, they showed some aspects of the myofiber structure disruption caused by lovastatin treatment using immunostaining against fast myosin heavy chain. It should be noted that these papers followed the effects of statin treatment in embryos at 24 hours post-fertilization (hpf), when most of the muscle differentiation is already completed. Therefore, their work does not focus on muscle commitment or differentiation, which is our main interest.

We sought to study in detail the structural consequences of simvastatin treatment in zebrafish muscle formation. We previously demonstrated several gross structural and physiological effects of simvastatin treatment in zebrafish, and here we did a complete structural analysis of how myogenesis is affected. We wanted to analyze which of the components of the cytoskeleton/adhesion structures that are involved in myogenesis are affected by cholesterol withdrawal. The characterization of the muscular response to the administration of the drug will contribute to understanding of normal muscle development. Further, this work reaffirms the use of zebrafish as a model for statin-induced myopathies, and contributes to the understanding of the mechanisms of action of the statins.

Here, we describe the major alterations to the structure of the skeletal muscle of zebrafish embryos induced by simvastatin in a dose-dependent manner, particularly in terms of its effects on the distribution of matrix and adhesion components. Contributing to the understanding of the mechanism of action of the drug, we show that simvastatin structural effects could be rescued with cholesterol treatment.

Materials & Methods

Zebrafish Maintenance

Adult, wild-type *Danio rerio* fish were kept in a 14-hour light cycle in a system water at 28°C, according to standard procedures (Westerfield 2000). We developed our own zebrafish system, with several independent 7-L tanks, central water processing and with mechanical, biological and active carbon filters. Temperature was controlled by air-conditioning and water heaters. Embryos were collected from our wild-type colony, bleached with 0.05% NaOCl for 3 min and raised in system water. Fish were from the Fish Facility in the Institute of Biomedical Sciences of the Federal University of Rio de Janeiro, and all the procedures were approved by the Health

Sciences Center Ethics Committee for the Use of Animals in Research Federal University of Rio de Janeiro (Comissão de Ética no Uso de Animais em Pesquisa do Centro de Ciências da Saúde, CEUA-CCS, da Universidade Federal do Rio de Janeiro; DAHEICB 012).

Simvastatin Treatment

Embryos were dechorionated at 6 hpf and 11 hpf and placed in 100-mm Petri dishes filled with 50 ml of egg water (60 mg/l sea salts and 0.15% methylene blue). Embryos were treated with the following different concentrations of simvastatin: 0.3 nM, 3 nM, 6 nM, 0.375 μM, 0.5 μM, 0.75 μM, 1 μM, 2 μM and 10 μM. Embryos were treated with simvastatin for 18 hr or 13 hr at 28°C until they completed 24 hpf and then were processed as necessary. Simvastatin was dissolved in ethanol (final concentration of 0.02%).

Cholesterol-LDL Treatment

Embryos at 6 hpf were dechorionated and placed in 100-mm Petri dishes filled with 50 ml of egg water. Embryos were divided in the following four groups of treatments: (1) Embryos placed in egg water only; (2) Embryos placed in egg water containing 10% low density lipoprotein (LDL), with a ratio of 1:1500 molecules between LDL:cholesterol; (3) Embryos placed in egg water containing 0.3 nM simvastatin; (4) Embryos placed in egg water containing 0.3 nM simvastatin and 10% LDL with a ratio of 1:1500 molecules between LDL:cholesterol. All solutions were replaced by fresh egg water when embryos had completed 24 hpf.

Immunofluorescence

As described previously (Costa et al. 2008), embryos were dechorionated and fixed in methanol at -20°C overnight or with 4% formaldehyde in PBS at 5°C overnight. They were permeabilized with 0.5% Triton X-100 in PBS (PBS-T) for 30 min, and incubated for 1 hr at 37°C with a primary antibody. After a 30-min wash with PBS-T, embryos were stained with the secondary antibody. The nuclei were stained with 0.1 μg/ml DAPI in 0.9% NaCl. Specimens were washed for 5 min with 0.9% NaCl and mounted in PBS containing 0.1% sodium azide. All reagents were purchased from Sigma-Aldrich (St Louis, MO), unless otherwise stated. Control experiments of embryos stained with secondary antibodies showed no significant staining.

Antibodies and Fluorescent Probes

Primary antibodies were all purchased from Sigma-Aldrich: rabbit polyclonal anti-desmin (D-8281), mouse monoclonal anti-sarcomeric alpha-actinin (A-7811), rabbit polyclonal anti-laminin (L-9393) and mouse monoclonal anti-vinculin (V-4505). Alexa Fluor 488-goat anti-mouse/rabbit IgG, Alexa Fluor 546-goat anti-mouse/rabbit IgG antibodies and the DNA-binding probe, DAPI (40, 6-Diamidino-2-phenylindole dihydrochloride), were from Molecular Probes (Carlsbad, CA).

Optical Microscopy and Imaging

Embryos were visualized using a Zeiss Axiovert 100 inverted microscope (Zeiss; Oberkochen, Germany) using appropriate filters for fluorescence. Images were acquired with an Olympus DP71 high-resolution camera (Olympus; Tokyo, Japan). Images were also acquired with a disk confocal Olympus DSU mounted on an Olympus IX80 inverted microscope (Olympus) using appropriate filters for fluorescence. Images were processed with the ImageJ software, based on the public domain NIH Image program (developed at the U.S. National Institutes of Health and available on the Internet at http://rsb.info.nih.gov/nih-image/). The amount of protein in the images was estimated by the relative amount of fluorescence in each condition, assuming that it is proportional to the amount of antibody bound to the embryo. Therefore, the total gray level of the sum of 16 confocal slices for 3 consecutive somites in each condition was quantified with ImageJ. Plates were prepared using Adobe Photoshop (Adobe Systems Inc.; San Jose, CA).

Transmission Electron Microscopy

The dechorionated embryos were washed gently in warm PBS, pH 7.2, and fixed overnight in 2.5% glutaraldehyde, 4% formaldehyde and 5 mM $CaCl_2$ in 0.1 M cacodylate buffer (pH 7.2), and were then post-fixed for 90 min in 1% OsO_4 in 0.1 M cacodylate buffer containing 5 mM $CaCl_2$ and 0.8% potassium ferricyanide. Embryos were then dehydrated in acetone and embedded in Epon. Ultra-thin sections were cut and stained with uranyl acetate and lead citrate, and analyzed using a JEOL 1210 transmission electron microscope (Jeol; Tokyo, Japan).

Statistical Analysis

All values are the mean ± SD. Statistical comparisons were performed by unpaired *t*-tests for comparisons between two groups. In some cases, a one-way analysis of variance followed by Bonferroni post-hoc comparisons was used to analyze the differences between each group. Statistical significance was defined as $p<0.01$.

Results

We previously have shown that simvastatin added to fish water causes dose-related mortality rates and varied developmental defects (unpublished observations). We observed that high simvastatin doses (above 2 μM) in zebrafish embryos

induces fast lethal effects and profound morphological alterations whereas low simvastatin doses (0.3 nM) cause almost no lethality, no conspicuous gross morphological alterations (in a superficial assessment) but some physiological alterations. To better understand the structural aspects of myogenesis, we decided to further analyze the structural organization of simvastatin-treated zebrafish embryos

Structural Analysis of Changes Induced by Low-dose Simvastatin Treatment

The low (0.3 nM) simvastatin concentration did not produce any grossly abnormal phenotypes, but caused impairment in physiological responses, such as body movement and heartbeat. Therefore, we decided to analyze these embryos more carefully. Zebrafish embryos were treated with 0.3 nM simvastatin, cholesterol, or simvastatin + cholesterol for 18 hr and stained with antibodies against the myofibrillar protein alpha-actinin and the extracellular matrix protein laminin, and the nuclear dye DAPI (Fig. 1). In control embryos, alpha-actinin can be seen in myotomes in the somites of the whole embryo (red staining; Fig. 1A and, in progressively higher magnification, 1B and 1C, and Movie 1), whereas laminin is present in the chevron shaped-septa along the anterior-posterior axis of the embryos (Fig. 1A–C, green). In contrast, embryos treated with low doses of simvastatin showed faint alpha-actinin striations in shorter myofibrils, and there are gaps between the myofibrils (Fig. 1D–1F, red). Embryos treated with lower doses of simvastatin showed septa that continuously stained positively for laminin, although their shape is altered, and they do not exhibit the typical chevron pattern, but rather a smoother curve, with a larger angle (Fig. 1E–1F, green). The alterations in septa angle are probably related to the reduced contractile capability of the treated cells, as well as the loss of sarcomeric proteins in the muscle cells of the somites. Embryos treated with cholesterol alone have a distribution of myofibrils and septa similar to control, although the gap between the myofibrils is reduced, and the myofibrils are more aligned to the body axis (Fig. 1G–1I). Embryos submitted to treatment with both simvastatin and cholesterol showed a myofibrillar staining of alpha-actinin in a pattern similar to that of the control embryos, though not as regular (Fig. 1J–1L). Laminin staining in embryos treated with both simvastatin and cholesterol showed chevron-shaped septa (Fig. 1J–1L). To better appreciate the relative amount of expression of the muscle-specific myofibrillar marker, we quantified the relative amount of fluorescence in each condition, assuming that it is proportional to the amount of antibody bound to the embryo. We calculated that the protein expression in the simvastatin-treated somites was 34% ± 1% of the control, whereas the expression in the rescued embryos treated with simvastatin and the cholesterol complex was 56% ± 5% of the control. Embryos treated with the cholesterol complex alone expressed 83% ± 10% of the control fluorescence amount. These numbers confirm the extent of the differences, and show that simvastatin induces a reduction in the amount of proteins in the myofibrils and/or a reduction in the amount of differentiated muscle cells. Furthermore, the results confirm that cholesterol could compensate for the structural defects induced by simvastatin in the somites and septa of zebrafish embryos.

Observing these embryos at higher magnifications in single confocal sections, it is possible to follow individual myofibrils in all of the treatment conditions. Control embryos (Fig. 1C) show nicely striated multinucleated myotubes that are attached to straight septa that form a sharp angle in the middle line. Simvastatin-treated embryos show curved septa, with myofibrils with less stain and thinner than control (Fig. 1F). Nevertheless, these myotubes are striated and multinucleated. Interestingly, the cholesterol alone-treated embryos showed a very abundant myofibrillar stain, with marked striations (Fig. 1I) and the cholesterol-rescued embryos showed an intermediate amount of myofibrillar stain, with a normal straight angle of the septa (Fig. 1L).

Structural Analysis of Severe Phenotypes Induced by High-dose Simvastatin Treatment

A high (0.75 μM) simvastatin concentration led to high mortality rates and severely affected phenotypes. To better characterize the structural changes induced by simvastatin and to study how these alterations correlate with simvastatin dosage, we decided to study the skeletal muscle morphology of severely affected phenotypes caused by high doses of simvastatin. Again, we analyzed the organization of myofibrils and septa using confocal microscopy (Figs. 2 and 3, Movies S1, S2 and S3). Zebrafish embryos were treated with 0.75 μM simvastatin for 18 hr, fixed at 24 hpf, and stained with antibodies against alpha-actinin and laminin (Fig. 2A–2F). Since the body axis in treated embryos is compressed, somites in treated embryos (Fig. 2D–2F; Movie 4) are thicker and shorter than those in the control (Fig. 2A–2C, Movie 1). An increase in width can be seen by comparing the control embryo (Fig. 2B–2C) with somites of the treated embryos (Fig. 2E–2F) in the transversal, Y–Z axis reconstructions (Fig. 2B, 2E) and in sagittal, X–Z axis reconstructions (Fig. 2C, 2F). Not only were the treated somites shorter but the overall number of cells in each treated somite seemed to be reduced, as shown by DAPI nuclei staining (Fig. 3). Some apoptotic nuclei could be seen closer to the surface of the treated embryos. Treated muscle cells showed no myofibrils at all, or they were shorter and much thinner than those of the control, along several focal planes. This could be seen clearer in the projection of all focal planes of the confocal stack for the

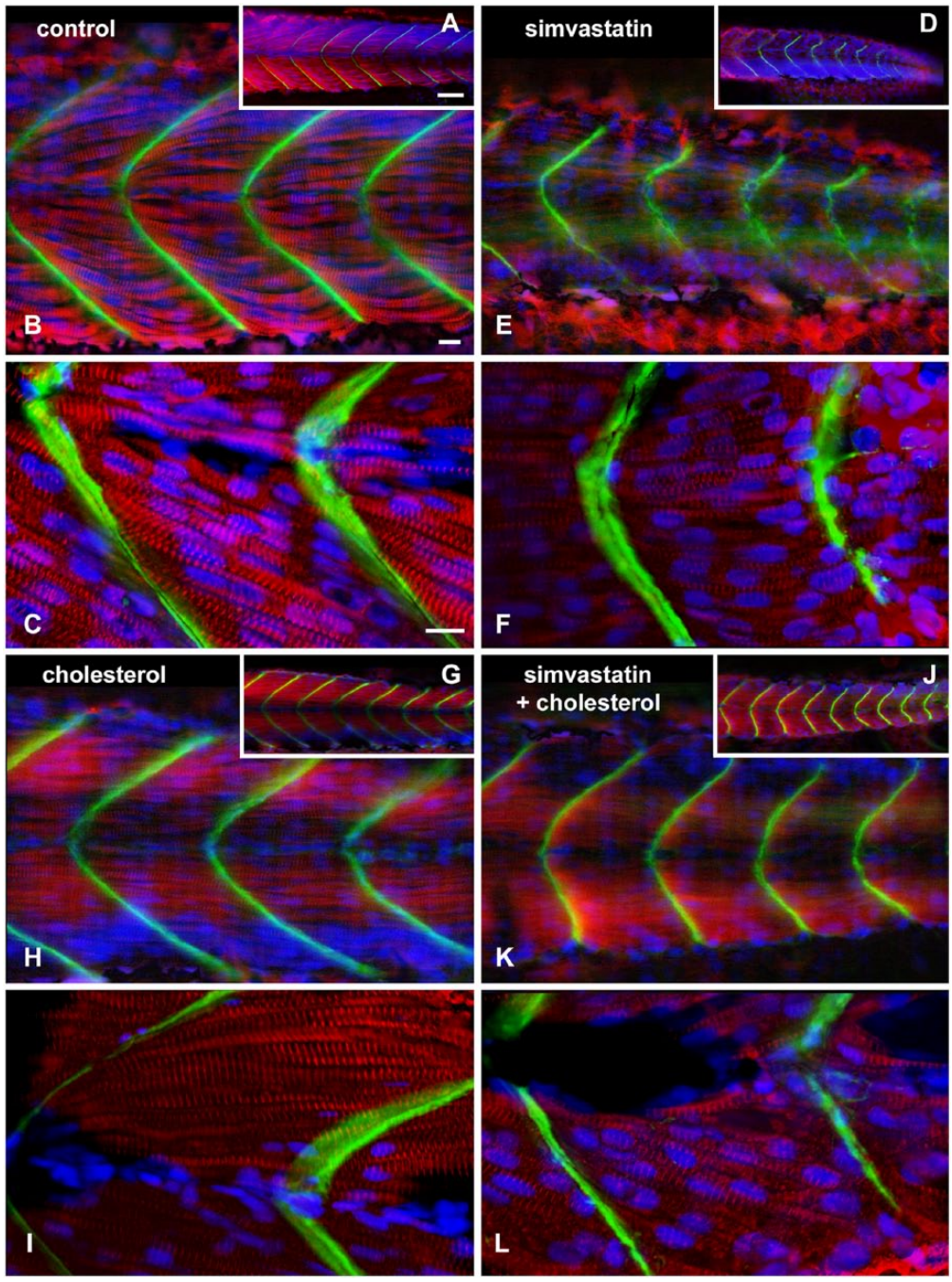

Figure 1. Structural analysis of mild phenotype, and its rescue with cholesterol. Confocal analysis of zebrafish embryos at 48 hours post-fertilization stained with sarcomeric alpha-actinin (red), laminin (green) and DAPI (blue). In the control embryo, a single slice shows eight regularly sized somites with straight angle septa (A). In the 0.3 nM simvastatin-treated embryo (D), there is a weak alpha-actinin stain, showing altered somites. In embryos treated with cholesterol alone (G), the somites appear regular in size. In embryos treated with simvastatin and cholesterol (J), the sizes of the somites are more similar to that of the control embryos than the embryos treated with simvastatin alone, although the septa are still irregular. In a projected region of six sequential slices (B, E, H and K), we can appreciate the continuity of the septa in the control embryos (B) and the embryos treated with cholesterol alone (H), whereas, in the simvastatin group, the septa is discontinuous and irregular (E). Simvastatin embryos rescued with cholesterol (K) show a more continuous septa than embryos treated with simvastatin alone, although these patterns are still not as regular as that in the control. At higher magnification (C, F, I and L), the striations are clearly seen in the straight myofibrils in control embryos (C) and embryos treated with cholesterol alone (H). In simvastatin-treated embryos (F), the myofibrils are shorter, curved and have a reduced stain for alpha-actinin. Embryos treated with simvastatin and cholesterol (L) have more alpha-actinin in striated myofibrils than simvastatin alone. Scale (A, D, G, J), 50 μm; (B, C, E, F, H, I, K, L), 10 μm.

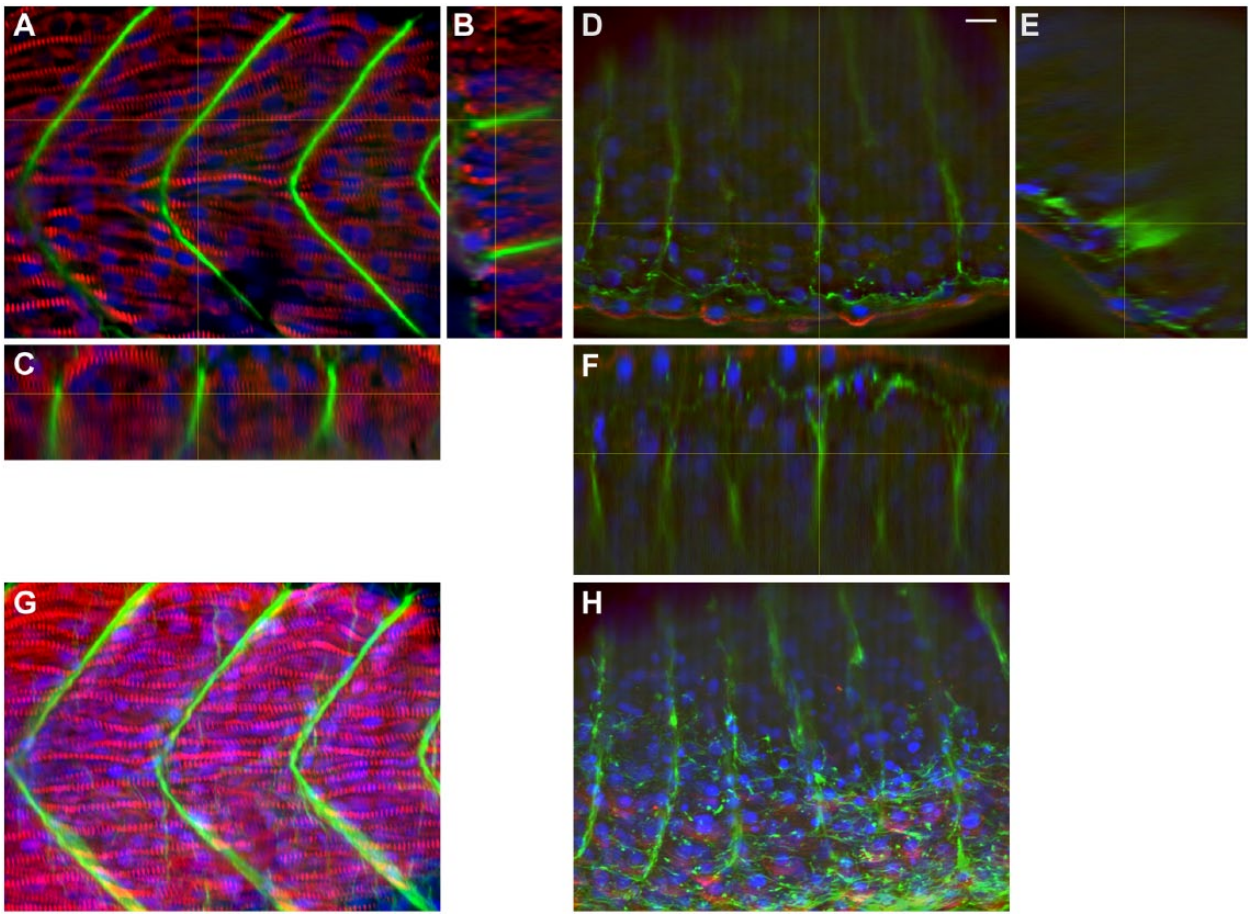

Figure 2. Structural analysis of severe phenotype: Myofibrils and septa. Confocal analysis of zebrafish embryos at 24 hours post-fertilization (hpf) stained with sarcomeric alpha-actinin (red), laminin (green) and DAPI (blue). In a control embryo, a single representative slice through somite 15 (A) is compared with orthogonal Z sections (B, C), and show perfectly striated myofibrils, with aligned nuclei and thick, continuous septa. In the 0.75 μM simvastatin-treated embryo (D), there is weak alpha-actinin stain, with faint laminin septa. The orthogonal sections (E, F) were cut through a region with laminin accumulation, stressing the discontinuity of the labeling. Note that the treated embryo (E, F) is thicker than the control (B, C; each slice in the confocal stack is 2 μm apart). Although the detail of the striation of the myofibrils is clearer using a single slice, the projections of the stacks (G, H) emphasize the regularity of the distribution of myofibrils and septa in the control (G), and the short somites divided by small amounts of laminin, sometimes in clumps, in the treated embryos (H). Scale, 10 μm.

control (Fig. 2G) and treated embryos (Fig. 2H). Whereas the septa run continuously from the outside to the inside of the embryo in controls, they seem to be discontinuous in the treated embryos, at least in some regions (note the Y–Z section in Fig. 2E). Laminin was found in the septa of both control and simvastatin-treated embryos, but treated embryos showed a thinner septum, with less laminin.

We also stained for the adhesion protein vinculin and the muscle-specific intermediate filament desmin. The accumulation of vinculin (red) was affected to the same extent as laminin (Fig. 3A, 3B). The desmin image (green) shows the same reduced staining aspect in the somite as observed for alpha-actinin, but also shows an accumulation in the remains of the septa along the vinculin staining. Occasionally, a thin myofibril in the simvastatin-treated embryos can be seen to stain positively for desmin and, interestingly, with clearly visible striations (Fig. 3G, arrow); this is compared with conspicuous striations of myofibrils (stained with alpha-actinin) in the control embryos (Fig. 2A). In control embryos, desmin is continuously distributed from top to bottom around the septa (Fig. 3C–3E), and is clearly concentrated around the nuclei. In treated embryos, desmin is present in clusters in the septal region, and there is an accumulation around the remnants of the septa (Fig. 3H, arrow). Desmin in wild-type embryos is distributed both in the myofibrils and in adhesion regions (Costa et al. 2004), and simvastatin treatment alters both distributions. In some places, an accumulation of vinculin can be seen where the septa is missing (Fig. 3G, arrowhead). The distribution of the nuclei is altered in simvastatin-treated embryos: Whereas the

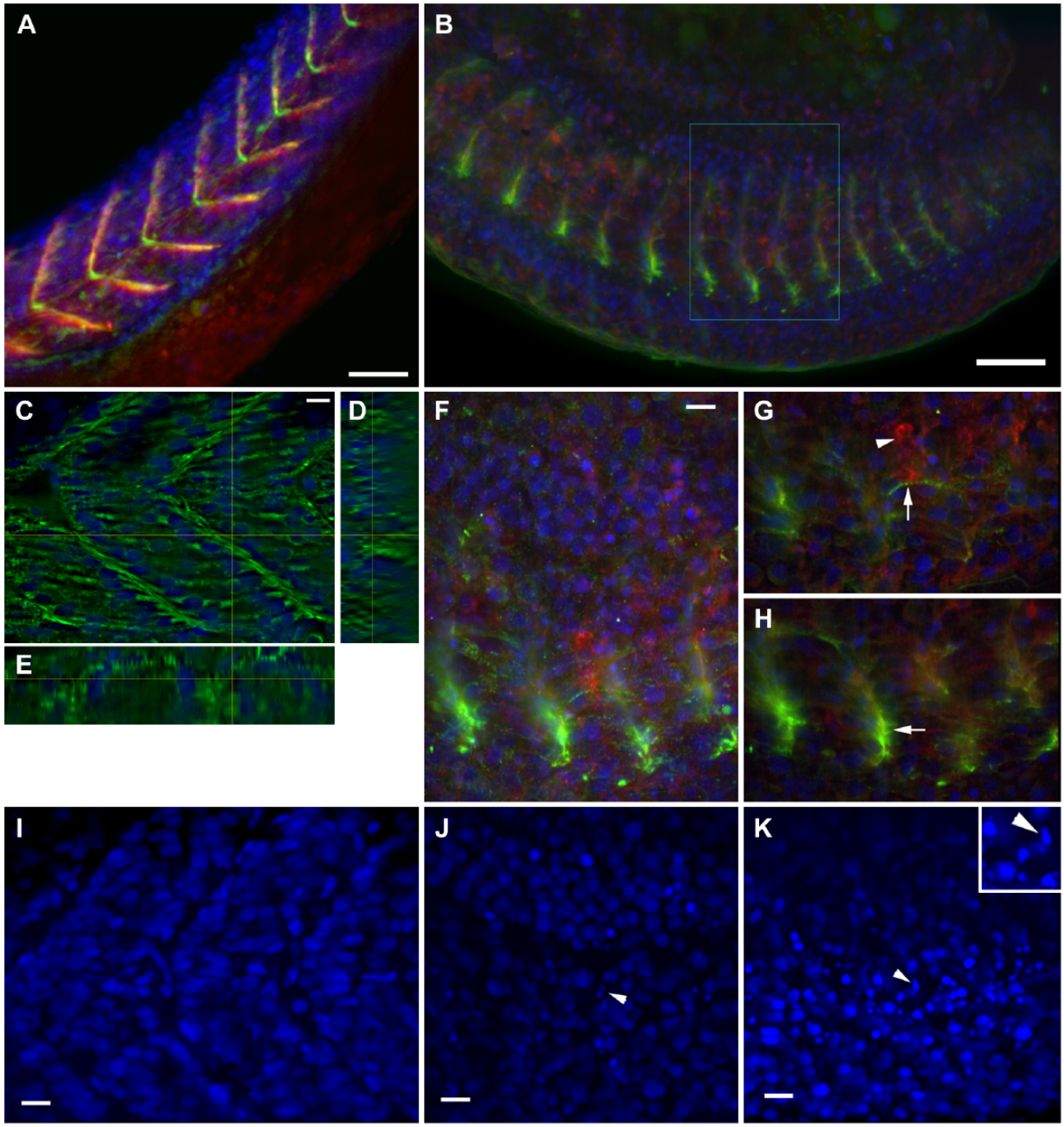

Figure 3. Structural analysis of severe phenotype: Intermediate filaments and adhesion complexes. Confocal analysis of zebrafish embryos at 24 hours post-fertilization (hpf) stained with desmin (green), vinculin (red) and DAPI (blue). Control embryo shows septa in chevron and large, regularly spaced somites in the stack projection (A). In the confocal projection of a 0.75 μM simvastatin-treated embryo (b), somites are shorter and septa labeling with vinculin is fainter, as is the myofibrillar desmin stain. In some regions, there is a small accumulation of desmin around the remnants of a septa (B). Analyzed in more detail, a selected slice of a control embryo shows the distribution of desmin around the nuclei, which are regularly spaced, and around the septa (C). The orthogonal sections show the septa (D) and a myofibril (E). In a detail of the inset in (B), the confocal projection highlights the concentration of desmin and vinculin staining (f). A selected slice (g) of the previous stack show a thin myofibril stained for desmin (arrow) close to an aggregate of vinculin (arrowhead). Another selected slice (h) shows the desmin accumulation in the remainder of the septum (arrowhead). In a projection of a DAPI labeling of control embryos (I), the gap where the septa lie is clearly visible. In the projections of treated embryos (J, K), the gap between the nuclei is not visible, and some apoptotic nuclei can be seen (arrowheads). This is clearer in the magnified inset in (K). Scale (A, B) 50 μm; (C, F, I, J, K) 10 μm.

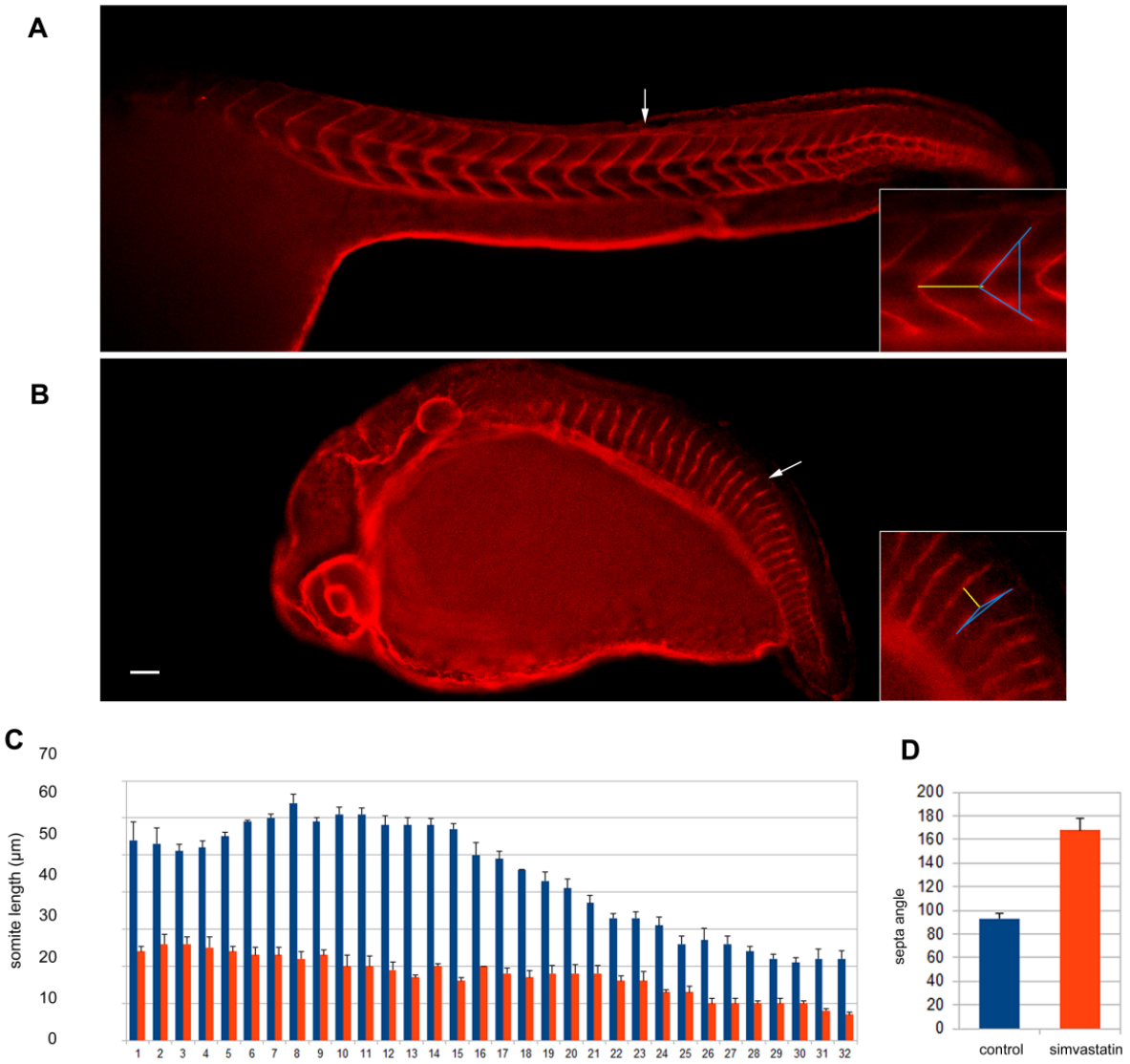

Figure 4. Quantification of simvastatin induced-structural changes. Using laminin staining in control (A) and treated (B) embryos, the size of each somite was measured and plotted, along with standard deviation in (C). The angle between the upper and lower part of the septa of somite 15 was also measured and compared (D). Significant differences in the mean levels were found between the 0.75 µM simvastatin-treated group and the control group ($p<0.01$; unpaired *t*-test). At least 10 embryos were used for each different experimental condition. Scale (A–B), 50 µm. The arrows point to somite 15, which are enlarged in the insets. The yellow line in the insets measures 56 µm in (A) and 18 µm in (B). The blue line indicates the septa angle of 83° in (A) and 162° in (B).

control embryos do not have nuclei in the septal region (Fig. 3I), treated embryos have the nuclei less organized and sometimes pyknotic (Fig. 3J–3K).

To better understand the overall body effects in terms of the somite-specific details we have been describing, we decided to quantify the total number and size of the somites and the angle of the septa of untreated and simvastatin-treated embryos with severe phenotypes (Fig. 4). Zebrafish embryos were treated with 0.75 µM simvastatin for 18 hr, fixed at 24 hpf, stained with the septa marker laminin and analyzed in a confocal microscope. No differences were found in the total number of somites comparing untreated and treated embryos. Both control and simvastatin-treated embryos had a total of 32 somites. In control embryos, the size of the somites varied along the anterior-posterior (A-P) axis, where the longer somites are located in the anterior region of the embryos. Our measurements of somite size of control embryos (Fig. 4C) are in accordance with the description of Schröter and colleagues (Schröter et al. 2008). We found a significant reduction in the size of the somites in the simvastatin-treated

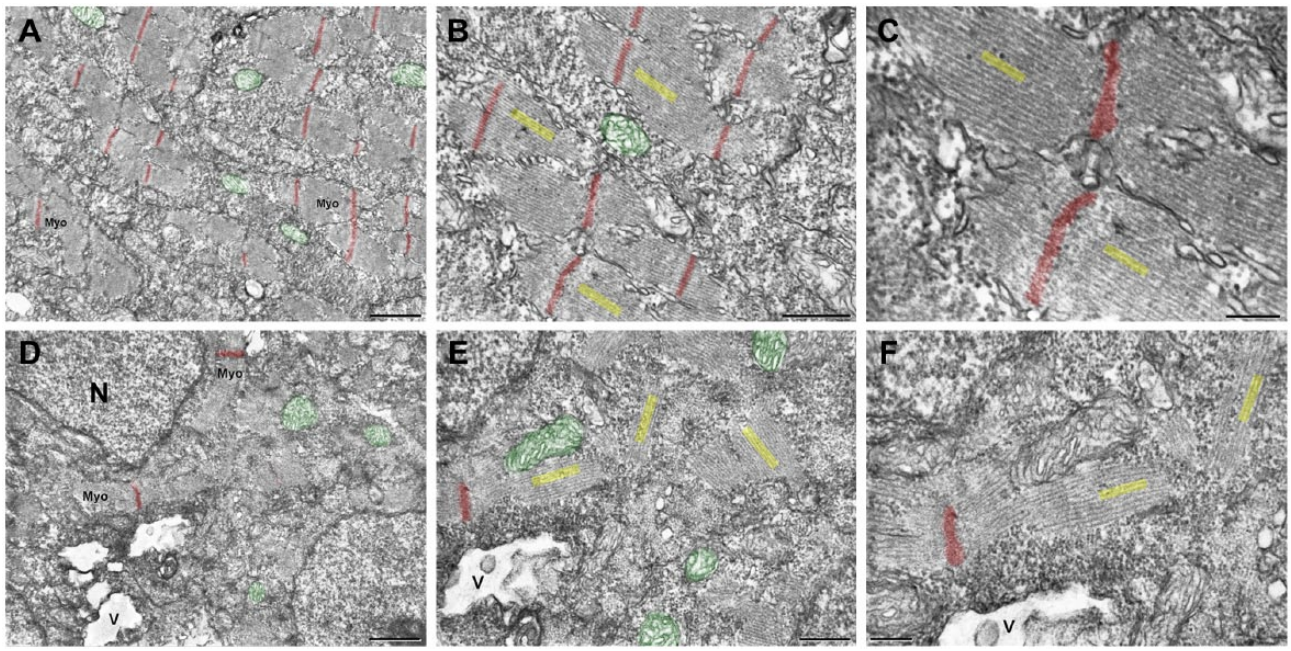

Figure 5. Transmission electron microscopy of zebrafish embryos treated with simvastatin. The untreated embryos (A–C) present organized bundles of myofibrils (Myo), and exhibit well-preserved mitochondria (green). Note that the Z lines (red) are aligned to each other and periodically spaced. The myofibrils around a Z-line are better visualized in figures (B, C), and their direction is indicated in yellow, showing their alignment. In the simvastatin-treated embryos (D–F), myofibrils (Myo) are disorganized and the alignment of Z lines is lost. Vacuoles (V) are observed, as well as several mitochondria (green) and nuclei (N). At a higher magnification (E, F), the myofibrils are clearly oriented in several directions (yellow). Note that, even when though the myofibrils are not aligned, the thick and thin filaments, marked in yellow within each myofibril, are parallel to each other, as happens in control. Scale (A, D) 1 μm; (B, E) 500 nm; (C), 200 nm; (F), 250 nm.

embryos as compared to control embryos. Furthermore, not only were the somites shorter, but there was a smaller variation in their size along the A-P axis. For example, somite number 15 measured 58 μm in untreated embryos and 18 μm in simvastatin-treated embryos, which comes to a 68% reduction in size. We also measured the angle of the septa in untreated and treated embryos (Fig. 4D). Control embryos showed an average angle of the septa of 93º ± 10º, whereas simvastatin-treated embryo showed an angle of 168º ± 5º. The high standard deviation values found in the control embryos are due to a normal gradual increase in the angle of the septa along the A-P axis. These results allowed us to define more precisely the structural changes induced by simvastatin in the somites and septa of zebrafish embryos.

Structural Analysis of Severe Phenotypes Induced by High-dose Simvastatin Treatment: Transmission Microscopy

To better understand the structural basis of the affected phenotype, we analyzed the muscle structure using transmission electron microscopy. Control embryos fixed at 24 hpf showed well-preserved mitochondria (colored with green), and well-organized and aligned myofibrils (colored with yellow) with sarcomeres and Z lines (colored with red) that run periodically perpendicular to the cell axis, even in separated myofibrils (Fig. 5A–5C, progressive magnifications). Embryos treated with a high dose simvastatin for 18 hr and fixed at 24 hpf, have large vacuoles, and degraded myofibrils (Fig. 5D–5F). The shorter myofibrils were interrupted and not aligned to each other or to the cell axis, and the Z lines were out of register. Interestingly, the thick and thin filaments were aligned to each other both in the control and treated muscles, and were still attached to the Z-lines (Fig. 5C, 5F). Some models of Z-line misalignment have been studied in zebrafish. For instance, this defect can be induced by knockdown of chaperone proteins (Codina et al. 2010; Bernick et al. 2010), which are known to participate in Z and M line assembly. Interestingly, Z-line misalignment has also been reported in desmin knockout mice (Li et al. 1997). These results demonstrate, at the sub-cellular level, how muscle structure is altered by simvastatin.

Discussion

We wanted to study the consequences of simvastatin in the structure and formation of zebrafish muscle. Simvastatin in low doses causes different effects to high doses.

When we analyzed in detail the structure of embryos treated with low simvastatin doses, which had no gross structural alterations, we showed subtle morphological changes, such as gaps between the myofibrils and a disturbed chevron shape. In these embryos, the septa of treated embryos were altered, with less continuous labeling for laminin. The myotomes displayed a fainter staining for myofibrillar proteins than observed in the control, suggesting either diminished amounts of protein or lower cell numbers. High simvastatin concentrations caused a severely disrupted phenotype, with a large reduction in embryo size, besides the septa and somite alterations. In these embryos, we also found a significant reduction in the size of the somites, which correlates with the overall body shortening observed. When we analyzed the size of each somite separately, we observed that the somites in treated embryos tended to have a similar size along the whole body axis, contrary to controls, where the anterior 5–10 somites tended to be larger. Shortened body axes are found in mutants with altered signaling pathways, such as Wnt/β-catenin and Shh, and in mutants with altered extracellular matrix proteins, such as laminin (Pollard et al. 2006, Parsons et al. 2002). In a more detailed investigation of the structure of the somites in simvastatin-treated embryos, we observed that the muscle cells were shorter and thinner with larger spaces between them, as compared with control embryos. The septa itself was also altered, and did not display a continuous distribution of laminin, as shown by the three-dimensional reconstruction of confocal images. We observed a larger accumulation of both vinculin and desmin around the remaining septa. It is interesting to note that both the extracellular (laminin) and intracellular (vinculin and desmin) components seemed to be affected in the same way (compare the laminin spot in Fig. 2E with the desmin/vinculin spot in Fig. 3H). We previously described adhesion structures composed of actin microfilaments, intermediate filaments (desmin), cellular adhesion proteins (vinculin) and extracellular proteins (laminin) during the normal development of zebrafish (Costa et al. 2002; Costa et al. 2008). The fact that their distribution is equally altered by simvastatin suggests a physical and functional link between their components.

The mevalonate metabolite dolichol phosphate is an important co-factor for the N-glycosylation of glycoproteins, which is required for their proper secretion to the extracellular space (Thorpe et al. 2004). We can speculate that simvastatin inhibits the glycosylation and secretion of extracellular glycoproteins, such as laminin, which impairs the proper formation of the septa in zebrafish embryos. The septa are part of the extracellular space that lies between two adjacent somites and it is composed by extracellular matrix and a few fibroblasts. The septa are important for the proper attachment of muscle cells for the generation of tension for muscle contraction. Simvastatin-treated embryos showed a reduction in the angle of septa, which could be related to the ability of muscle cells of the somites to contract and develop tension. Further experiments with later developmental stages, particularly with fluorescence-tagged live zebrafish embryos, could help to understand the relationship between septa and somites with statin treatment.

The alterations we showed in the distribution of adhesion protein structures could be caused by membrane microdomain alterations induced by simvastatin treatment. Components of the microdomains have been shown to change in distribution during myogenesis (Draeger et al. 2010). It will be interesting to demonstrate a direct relationship between affected areas and microdomain markers. It is also possible that the effects reported here are indirect, toxic consequences of simvastatin, which probably affects other tissues besides muscle (Baek et al. 2012).

To test if the simvastatin effects observed here were caused by cholesterol withdrawal and not by other molecules, we sought to rescue the statin-induced phenotype with cholesterol. We showed that concentrations of cholesterol that do not seem to have adverse effects on the embryos by themselves are sufficient to recover the damage caused by simvastatin. Interestingly, the structure of the myofibrils in the cholesterol-treated embryos was not completely normal. It will be interesting to use zebrafish as a model of hypercholesterolemia, and to see the effects of simvastatin in these animals. The fact that cholesterol can rescue most of the statin effects suggests that other pathways related to HMG-CoA reductase could also be affected, suggesting that there are other pathways involved. For instance, statins have been shown to inhibit farnesylation and geranylgeranylation of proteins (Cao et al. 2009). This could explain why not all of the effects of simvastatin were reversed with cholesterol. Further experiments should be done to test the role of other end-results in the cholesterol biosynthetic pathway, such as mevalonate and glycosylation inhibition.

Statins are effective in lowering the risk of cardiovascular problems but they cause several side effects. The range of dosages that we used here are comparable with the doses prescribed in the clinic. Here we show how simvastatin causes muscle damage, but further studies will be necessary to allow for an extrapolation of our results to human myopathies.

We studied the structural alterations caused by different concentrations of simvastatin treatment in terms of embryo and somite size, septa shape, and myofibril structure. These effects could be reversed by the addition of exogenous cholesterol. Our results show how statins affect the formation of the muscle cytoskeleton and adhesion, and highlight the advantages of the zebrafish model for the study of cholesterol in myogenesis.

Acknowledgments

We thank Livia Guapyassu for assistance and Sandra Regina Enrique Castro for handling the fish.

Declaration of Conflicting Interests

The authors declared no potential conflicts of interest with respect to the research, authorship, and/or publication of this article.

Funding

The authors disclosed receipt of the following financial support for the research, authorship, and/or publication of this article: This work was supported by the Conselho Nacional de Desenvolvimento Cientıfico e Tecnológico (CNPq), the Fundação Carlos Chagas Filho de Apoio à Pesquisa do Estado do Rio de Janeiro (FAPERJ) and the Programas de Apoio aos Núcleos de Excelência (Pronex).

References

Baek JS, Fang L, Li AC, Miller YI (2012). Ezetimibe and simvastatin reduce cholesterol levels in zebrafish larvae fed a high-cholesterol diet. Cholesterol 2012:564705

Bernick EP, Zhang P, Du S (2010). Knockdown and overexpression of unc-45b result in defective myofibril organization in skeletal muscles of zebrafish embryos. BMC Cell Biol 11:70.

Cao P, Hanai J, Tanksale P, Imamura S, Sukhatme VP, Lecker SH (2009). Statin-induced muscle damage and atrogin-1 induction is the result of a geranylgeranylation defect. FASEB J. 23:2844-2854.

Clark KA, McElhinny AS, Beckerle MC, Gregorio CC (2002). Striated muscle cytoarchitecture: an intricate web of form and function. Annu Rev Cell Dev Biol. 18:637-706.

Codina M, Li J, Gutiérrez J, Kao JPY, Du SJ (2010). Loss of smyhc1 or hsp90alpha1 function results in different effects on myofibril organization in skeletal muscles of zebrafish embryos. PLoS One. 5:e8416.

Costa M (2014). Cytoskeleton and adhesion in myogenesis. ISRN Developmental Biology. 2014:1-15.

Costa ML, Escaleira R, Cataldo A, Oliveira F, Mermelstein CS (2004). Desmin: molecular interactions and putative functions of the muscle intermediate filament protein. Braz J Med Biol Res 37:1819-1830.

Costa ML, Escaleira RC, Jazenko F, Mermelstein CS (2008). Cell adhesion in zebrafish myogenesis: distribution of intermediate filaments, microfilaments, intracellular adhesion structures and extracellular matrix. Cell Motil Cytoskeleton 65:801-815.

Costa ML, Escaleira RC, Rodrigues VB, Manasfi M, Mermelstein CS (2002). Some distinctive features of zebrafish myogenesis based on unexpected distributions of the muscle cytoskeletal proteins actin, myosin, desmin, alpha-actinin, troponin and titin. Mech Dev 116:95-104.

Draeger A, Sanchez-Freire V, Monastyrskaya K, Hoppeler H, Mueller M, Breil F, Mohaupt MG, Babiychuk EB (2010). Statin therapy and the expression of genes that regulate calcium homeostasis and membrane repair in skeletal muscle. Am J Pathol 177:291-299.

Engler AJ, Griffin MA, Sen S, Bönnemann CG, Sweeney HL, Discher DE (2004). Myotubes differentiate optimally on substrates with tissue-like stiffness: pathological implications for soft or stiff microenvironments. J Cell Biol 166:877-887.

Galbiati F, Engelman JA, Volonte D, Zhang XL, Minetti C, Li M, Hou HJ, Kneitz B, Edelmann W, Lisanti MP (2001). Caveolin-3 null mice show a loss of caveolae, changes in the microdomain distribution of the dystrophin-glycoprotein complex, and t-tubule abnormalities. J Biol Chem 276:21425-21433.

Hanai J, Cao P, Tanksale P, Imamura S, Koshimizu E, Zhao J, Kishi S, Yamashita M, Phillips PS, Sukhatme VP (2007). The muscle-specific ubiquitin ligase atrogin-1/mafbx mediates statin-induced muscle toxicity. J Clin Invest 117:3940-3951.

Henry CA, McNulty IM, Durst WA, Munchel SE, Amacher SL (2005). Interactions between muscle fibers and segment boundaries in zebrafish. Dev Biol 287:346-360.

Kaufmann U, Martin B, Link D, Witt K, Zeitler R, Reinhard S, Starzinski-Powitz A (1999). M-cadherin and its sisters in development of striated muscle. Cell Tissue Res 296:191-198.

Li Z, Mericskay M, Agbulut O, Butler-Browne G, Carlsson L, Thornell LE, Babinet C, Paulin D (1997). Desmin is essential for the tensile strength and integrity of myofibrils but not for myogenic commitment, differentiation, and fusion of skeletal muscle. J Cell Biol 139:129-144.

Mermelstein CS, Amaral LM, Rebello MIL, Reis JSN, Borojevic R, Costa ML (2005). Changes in cell shape and desmin intermediate filament distribution are associated with down-regulation of desmin expression in c2c12 myoblasts grown in the absence of extracellular ca2+. Braz J Med Biol Res 38:1025-1032.

Mermelstein CS, Portilho DM, Mendes FA, Costa ML, Abreu JG (2007). Wnt/beta-catenin pathway activation and myogenic differentiation are induced by cholesterol depletion. Differentiation 75:184-192.

Parsons MJ, Pollard SM, Saúde L, Feldman B, Coutinho P, Hirst EMA, Stemple DL (2002). Zebrafish mutants identify an essential role for laminins in notochord formation. Development 129:3137-3146.

Pollard SM, Parsons MJ, Kamei M, Kettleborough RNW, Thomas KA, Pham VN, Bae M, Scott A, Weinstein BM, Stemple DL (2006). Essential and overlapping roles for laminin alpha chains in notochord and blood vessel formation. Dev Biol 289:64-76.

Portilho DM, Soares CP, Morrot A, Thiago LS, Butler-Browne G, Savino W, Costa ML, Mermelstein C (2012). Cholesterol depletion by methyl-β-cyclodextrin enhances cell proliferation and increases the number of desmin-positive cells in myoblast cultures. Eur J Pharmacol 694:1-12.

Schröter C, Herrgen L, Cardona A, Brouhard GJ, Feldman B, Oates AC (2008). Dynamics of zebrafish somitogenesis. Dev Dyn 237:545-553.

Thorpe JL, Doitsidou M, Ho SY, Raz E, Farber SA (2004). Germ cell migration in zebrafish is dependent on HMGCoA reductase activity and prenylation. Dev Cell 6:295-302.

Tobert JA (2003). Lovastatin and beyond: the history of the hmg-coa reductase inhibitors. Nat Rev Drug Discov 2:517-526.

Westerfield M (2000). The zebrafish book. A guide for the laboratory use of zebrafish (*Danio rerio*). Eugene: University of Oregon Press.